Bioorganic & Medicinal Chemistry 26 (2018) 875–883

Contents lists available at ScienceDirect

Bioorganic & Medicinal Chemistry

journal homepage: www.elsevier.com/locate/bmc

Design, synthesis and fungicidal evaluation of novel pyraclostrobin analogues

Lili Wang [a,d], Shuangshuang Zhao [b,d], Xiaotian Kong [c], Lingling Cao [b], Sheng Tian [a,*], Yonghao Ye [b,*], Chunhua Qiao [a,*]

[a] Jiangsu Key Laboratory of Preventive and Translational Medicine for Geriatric Diseases, College of Pharmaceutical Sciences, Soochow University, Suzhou 215123, PR China
[b] College of Plant Protection, State & Local Joint Engineering Research Center of Green Pesticide Invention and Application, Nanjing Agricultural University, Nanjing 210095, PR China
[c] Institute of Functional Nano and Soft Materials (FUNSOM), Soochow University, Suzhou, Jiangsu 215123, PR China

ARTICLE INFO

Article history:
Received 22 November 2017
Revised 5 January 2018
Accepted 8 January 2018
Available online 10 January 2018

Keywords:
Antifungal activity
Pyraclostrobin analogues
Phytopathogenic fungi
Cytochrome bc_1 complex inhibitor
Molecular docking

ABSTRACT

A series of novel pyraclostrobin derivatives were designed and prepared as antifungal agents. Their antifungal activities were tested in vitro with five important phytopathogenic fungi, namely, *Batrylis cinerea*, *Phytophthora capsici*, *Fusarium sulphureum*, *Gloeosporium pestis* and *Sclerotinia sclerotiorum* using the mycelium growth inhibition method. Among these compounds, **5s** displayed IC_{50} value of 0.57 μg/mL against *Batrylis cinerea* and **5k-II** displayed IC_{50} value of 0.43 μg/mL against *Sclerotinia sclerotiorum*, which were close to that of the positive control pyraclostrobin (0.18 μg/mL and 0.15 μg/mL). Other compounds **5f**, **5k-II**, **5j**, **5m** and **5s** also exhibited strong antifungal activity. Further enzymatic assay demonstrated compound **5s** inhibited porcine bc_1 complex with IC_{50} value of 0.95 μM. The statistical results from an integrated computational pipeline demonstrated the predicted total binding free energy for compound **5s** is the highest. Consequently, compound **5s** with the biphenyl-4-methoxyl side chain could serve as a new motif as inhibitors of bc_1 complex and deserve to be further investigated.

1. Introduction

Pyraclostrobin (Fig. 1) belongs to the strobilurin type of fungicide.[1] Pyraclostrobin was believed to bind to the Q_o site of a membrane-bound homodimeric cytochrome bc_1 complex (EC 1.10.2.2, also known as complex III of mitochondrial respiration) and blocked the electron transfer between cytochrome b and cytochrome c1, resulting in the inhibition of the mitochondrial respiration chain and the reduced production of ATP which is essential for the proper function of fungal cell.[2] Ever since being introduced to the market by BASF,[3] pyraclostrobin has been playing critical roles in crop protection. After extensive application for over two decades, fungi phytopathogens with moderate to high resistance to pyraclostrobin have been reported.[4,5] Therefore, development of pyraclostrobin analogues for the treatment of resistant pathogens has been the efforts for the agricultural chemists.

As shown in Fig. 1, the structure of pyraclostrobin could be divided into three parts: the pharmacophore, the phenyl bridge and the side chain. The pharmacophore moiety exists in a number of highly potent strobilurin type fungicides,[6–17] variation at the side chain is observed in several marketed agents, while modification of the phenyl linker is rarely reported.[18–21] Considering phenyl is commonly replaced by its bioisostere pyridinyl, and the synthesis of *N*-ortho substituted pyridine analogues could be easily achieved by nucleophilic aromatic substitution reaction, we herein designed and synthesized a series of pyraclostrobin derivatives bearing the pyridinyl linker, and the side chain was accordingly investigated. The fungicidal activities of these compounds were evaluated against five important plant pathogen strains including *Batrylis cinerea*, *Phytophthora capsici*, *Fusarium sulphureum*, *Gloeosporium pestis* and *Sclerotinia sclerotiorum* in vitro, and the inhibitory capability against porcine bc_1 complex were evaluated. Finally, the structure-activity relationships (SARs) were also analyzed using integrated computational strategy including molecular docking, MM/GBSA binding free energy calculation and binding free energy decomposition.

2. Results and discussion

2.1. Chemistry

The synthesis of the target molecules **5a–u** and **6a–b** was started from the commercially available 2-chloro-3-nitropyridine

* Corresponding authors.
E-mail addresses: stian@suda.edu.cn (S. Tian), yeyh@njau.edu.cn (Y. Ye), qiaochunhua@suda.edu.cn (C. Qiao).
[d] These two authors contributed equally.

https://doi.org/10.1016/j.bmc.2018.01.004
0968-0896/

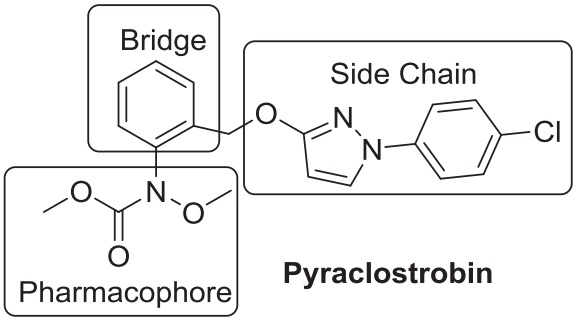

Fig. 1. Chemical structure of pyraclostrobin.

(Scheme 1). To prepare **1a**–**v**, the essential reaction intermediates 4′-chloro-(1,1′-biphenyl)-4-ol, 3′,4′-dichloro-(1,1′-biphenyl)-4-ol and 4-(pyridin-3-yl)phenol were prepared by Suzuki coupling reactions according to reported procedures.[22,23] Reaction intermediate (1-(4-chlorophenyl)-1*H*-pyrazol-3-yl)methanol was synthesized employing the reported method through a three-step procedure.[24] Reduction of the commercially available 5-(2,5-dichlorophenyl)furan-2-carbaldehyde using $NaBH_4$ afforded the alcohol intermediate (5-(2,5-dichlorophenyl)furan-2-yl)methanol. All other side chain fragments were from commercial sources. Nucleophilic aromatic substitution reaction of 2-chloro-3-nitropyridine with the above reaction intermediates using different base afforded the corresponding products **1a**–**v**. Treatment of **1k** with NaH in anhydrous THF followed by addition of iodomethane provided intermediate **2k**. Reduction of **1a**–**j**, **1l**–**v** and **2k** using stannous chloride in the presence of sodium acetate afforded the crude product hydroxylamines **3a**–**v**, which were immediately treated with methyl chloroformate at −10 °C to give the corresponding **4a**–**v** in good yields (60–83%). Methylation of **4a**–**v** with iodomethane in a sealed tube under basic condition (potassium carbonate in acetone) afforded the target molecules **5a**–**v** in 66–91% yields. The quaternary ammonium salt **5i** was obtained at the methylation step. Compounds **6a**–**b** were prepared through the classical click chemistry (copper-catalyzed azide–alkyne cycloaddition). Treatment of **5v** with the two azido compounds 1-(azidomethyl)-4-chlorobenzene and 1-azido-4-chlorobenzene[25,26] in the presence of hydrazine hydrate and copper(II) sulfate gave **6a**–**b**. All prepared compounds were analyzed by high-pressure liquid chromatography to ensure the purity (>98%) before submission for biological evaluation.

2.2. Antifungal activity

As shown in Table 1, the prepared twenty-three target compounds were divided into two different types. For type I compounds, the aryl ring is directly attached to the pyridone oxygen, while type IA (**5a**–**c**) distinguished from IB (**5d**–**k**) by the presence of only one aryl ring at the side chain. For type II compounds, the pyridone oxygen is attached to the aromatic ring through a methylene linker. In term of antifungal activity, all type IA compounds displayed poor antifungal activity. By comparison, Type IB compounds generally displayed improved antifungal activity. Specifically, compound **5k-II**, with *N*-methylcarbazole at the side chain, exhibited a broad spectrum of antifungal activity against all five tested phytopathogens. The inhibition rate (25 μg/mL) against *Fusarium sulphureum* and *Sclerotinia sclerotiorum* were 73% and 98%, comparable to that of the positive control pyraclostrobin (78% and 100%). Replacement of one or two hydrogen atoms with chlorine at the side chain lead to significantly decreased inhibition percentage, from 100% (**5f**) to 31% (**5h**) against *Sclerotinia sclerotiorum*, suggesting the chlorine atom on the side chain of type IB compounds could not be accommodated. Compound **5i**, with the quaternary ammonium side chain, exhibited less than 10% antifungal activity against all five tested fungi phytopathogens; while high inhibitory activity of **5f** and **5k-II** concluded that the electron rich hydrophobic side chain is favorable for the compounds antifungal activity. Compounds with benzyloxyl group at the 2-position of the pyridine ring were grouped as typeⅡ, while type IIA (**5l**–**r**) with a single aryl ring at the side chain distinguished from type IIB (**5s**–**5u**, **6a-ab**) with biaryl rings. As shown in Table 1, nine out of twelve typeⅡ compounds displayed moderate to good antifungal activity. Compound **5m** demonstrated the highest inhibitory potency against all tested fungi phytopathogens (inhibition rate between 43 and 100% at 25 μg/mL) in this group. Compound **5b**

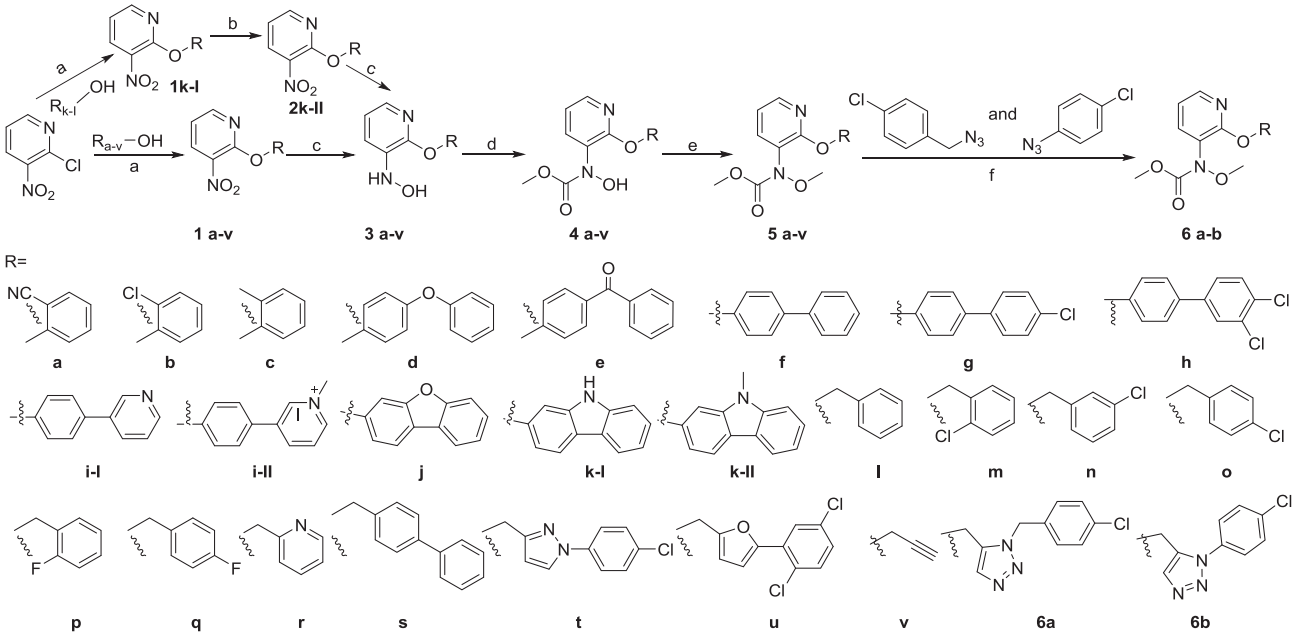

Scheme 1. Synthetic route of the target molecules **5a**–**v** and **6a**–**b**.

Table 1
Antifungal activity of the prepared compounds in vitro.

		NO.	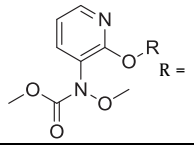	Percentage of inhibition (25 μg/mL)				
				Batrylis cinerea	*Phytophthora capsici*	*Fusarium sulphureum*	*Gloeosporium pestis*	*Sclerotinia sclerotiorum*
Type Ⅰ	Type ⅠA	**5a**	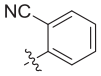	8	2	–	17	–
		5b		42	4	13	23	12
		5c		6	6	–	22	–
	Type ⅠB	**5d**	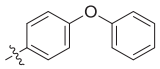	79	34	33	66	100
		5e	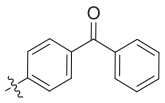	30	18	8	36	55
		5f	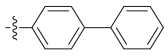	82	47	50	70	100
		5g	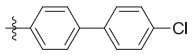	64	35	29	54	64
		5h	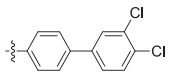	46	17	19	41	31
		5i	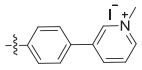	4	–	10	8	–
		5j	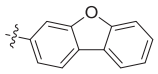	67	32	37	53	89
		5k-Ⅱ	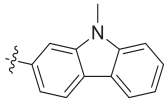	85	50	73	50	98
Type Ⅱ	Type ⅡA	**5l**	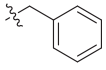	15	10	0	29	23
		5m	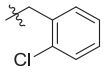	78	43	55	51	100
		5n	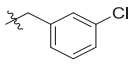	71	35	37	45	53
		5o	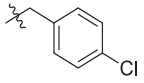	64	20	27	43	41
		5p	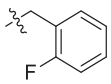	76	21	25	27	38
		5q	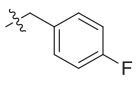	60	13	16	29	31

(*continued on next page*)

Table 1 (*continued*)

	NO.	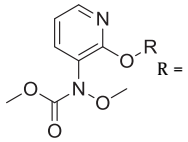	Percentage of inhibition (25 μg/mL)				
			Batrylis cinerea	*Phytophthora capsici*	*Fusarium sulphureum*	*Gloeosporium pestis*	*Sclerotinia sclerotiorum*
	5r	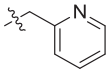	28	1	1	13	–
Type IIB	**5s**	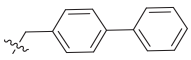	81	33	44	78	72
	5t	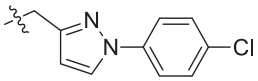	64	23	30	64	40
	5u	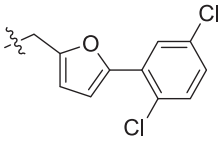	61	24	14	41	34
	6a	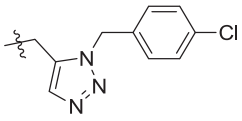	48	8	8	21	3
	6b	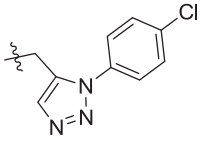	28	9	21	32	33
	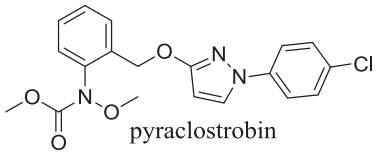 pyraclostrobin		100	100	78	87	100

–: No antifungal effect. The antifungal activity was determined using the mycelia growth inhibitory rate method.

Table 2
IC_{50} values of some selected compounds against the five tested phytopathogens.

NO.	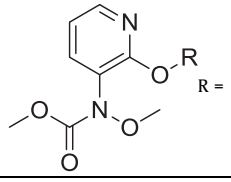	IC_{50} ± SD(μg/mL)[a]				
		Batrylis cinerea	*Phytophthora capsici*	*Fusarium sulphureum*	*Gloeosporium pestis*	*Sclerotinia sclerotiorum*
5d	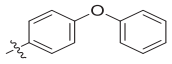	2.93 ± 0.03	12.92 ± 0.15	>25	>25	3.51 ± 0.11
5f	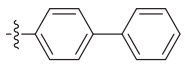	0.98 ± 0.02	7.51 ± 0.07	25.00 ± 0.30	25.61 ± 0.27	0.64 ± 0.03
5j	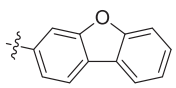	>25	>25	>25	>25	1.73 ± 0.05
5k-II	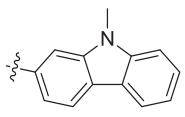	1.18 ± 0.13	24.78 ± 0.37	2.43 ± 0.13	24.56 ± 0.11	0.43 ± 0.02

Table 2 (*continued*)

NO.		IC_{50} ± SD(μg/mL)[a]				
		Batrylis cinerea	*Phytophthora capsici*	*Fusarium sulphureum*	*Gloeosporium pestis*	*Sclerotinia sclerotiorum*
5m	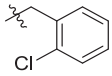	19.28 ± 0.3	>25	>25	>25	1.46 ± 0.04
5n	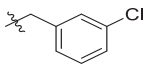	10.82 ± 0.1	>25	>25	>25	>25
5p	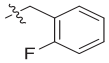	20.09 ± 0.2	>25	>25	>25	>25
5s	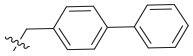	0.57 ± 0.01	>25	>25	ND	7.18 ± 0.09
pyraclostrobin	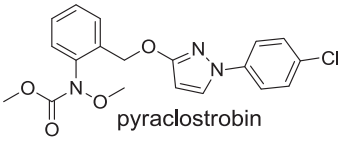	0.18 ± 0.05	0.005 ± 0.00	0.36 ± 0.03	0.03 ± 0.00	0.15 ± 0.01

[a] Values are the mean ± standard deviation (SD) of three replicates. ND: not determined.

Table 3
Percentage of inhibition, IC_{50} values and predicted total binding free energy of selected compounds against porcine SCR.

NO.		%Inhibition (100 μM)	IC_{50} ± SD (μM)[a]	ΔG_{pred}[c] (kcal/mol)
5b	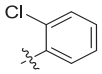	<10%	/[b]	−15.60
5d	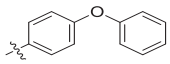	41%	/	−35.81
5e	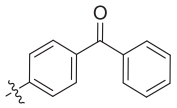	13%	/	3.30
5f	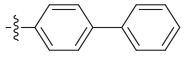	11%	/	−23.84
5g	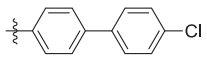	22%	/	−15.10
5k-II	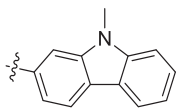	43%	/	−18.69
5m	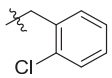	79%	32.14 ± 0.11	−37.87
5s	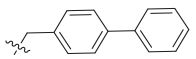	99.9%	0.95 ± 0.012	−44.17

(*continued on next page*)

Table 3 (*continued*)

NO.		%Inhibition (100 μM)	IC_{50} ± SD (μM)[a]	ΔG_{pred}[c] (kcal/mol)
	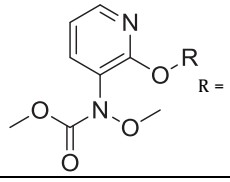 R =			
5t	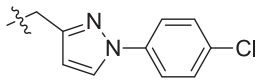	55%	38.84 ± 0.78	−34.15
	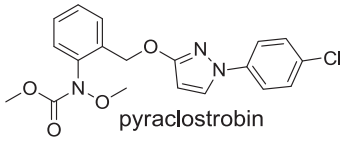 pyraclostrobin	99.9%	1.76 ± 0.17 nM	−35.85
	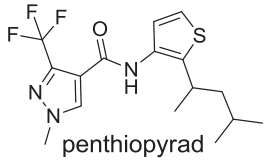 penthiopyrad	95%	1.56 ± 0.12	/

[a] Values are the mean ± standard deviation (SD) of three replicates.
[b] Not tested.
[c] The predicted binding free energies between each compound and cytochrome bc1 complex (PDB ID: 3TGU, ε_{in} = 1.0).

devoid of the methylene linker exhibited much lower antifungal activity, suggesting more flexible side chain is favorable for the antifungal activity. In addition, halogen atom on the phenyl ring in typeⅡA compounds could significantly increase the antifungal activity (**5l** *vs* **5m**–**q**), this is different from the type I compounds. Moreover, the chlorine atom on the phenyl ring is more appropriate than the fluorine atom, as demonstrated by comparing the activity of **5m** *vs* **5p**, and **5o** *vs* **5q**. Compound **5r** with pyridine ring at side chain displayed significantly decreased antifungal activity, and low inhibition activity similar to that of compound **5i** was observed. In general, the typeⅢB compounds (**5s**–**u**, **6a**–**b**) displayed antifungal activity close to that of typeⅡA compounds. Compound **5s** in this group exhibited the highest inhibitory potency against *Batrylis cinerea*, *Gloeosporium pestis* and *Sclerotinia sclerotiorum*, with inhibition percentage ranges from 72% to 81% at 25 μg/mL. Replacement of the phenyl ring with other five-member heterocycle (**5t**–**u**, **6a**–**b**) reduced the antifungal activity.

To analyze the antifungal effect more accurately, the IC_{50} values were further determined for compounds with inhibitory percentage higher than 50% at 25 μg/mL. The results were shown in Table 2. Compound **5f** and **5k-II** exhibited a broad spectrum of antifungal activity against the five tested phytopathogens. Especially, the IC_{50} values of **5f** (0.98 μg/mL against *Batrylis cinerea*) and **5k-II** (0.43 μg/mL against *Sclerotinia sclerotiorum*) were close to that of positive control pyraclostrobin (0.18 μg/mL and 0.15 μg/mL). Additionally, compound **5s** displayed strong antifungal activity against *Batrylis cinerea* with an IC_{50} value 0.57 μg/mL, which is comparable to that of pyraclostrobin (0.18 μg/mL). Generally, these compounds demonstrated higher fungicidal activity against *Batrylis cinerea* and *Sclerotinia sclerotiorum* than other three fungi phytopathogens.

2.3. Inhibition effect against bc_1 complex

To further understand the inhibition mechanism, representative compounds were selected for cytochrome bc_1 complex assay. The activity of the complex in the succinate-cytochrome c reductase (SCR) was determined using decylubiquinol (DBH2) and cytochrome c_1 as substrates.[27]

As shown in Table 3, compound **5s** exhibited the lowest IC_{50} value (0.95 μM) against porcine SCR, which is lower than the positive control penthiopyrad (95% at 100 μM, IC_{50}1.56 μM). In contrast, compound **5f** without the methylene linker displayed only 11% inhibitory activity at 100 μM, suggesting the flexible side chain is favorable for the enzymatic inhibition activity. This result is consistent with the cell based assay. The same trend was confirmed by comparing the inhibitory activity of **5m** (79%) with **5b** (<10%). Comparing the inhibitory activity of compound **5b** (<10%) with **5d**–**5k-II** (11–43%), it could be concluded that the presence of biaryl rings is more favorable than single aryl ring at the side chain, this conclusion is apparently also supported by the activity difference between compound **5m** (79%) *vs* **5s** (99.9%).

2.4. Structure-activity relationships (SARs) discussion

In order to demonstrate the detected biological activity difference, the representative compounds listed in Table 3 were docked into the binding pocket of cytochrome bc1 complex using standard precision (SP) and extra precision (XP) scoring functions in *Glide* docking. The statistical results from the *Glide* docking do not have satisfactory prediction capability for ranking the biological activities of the studied chemicals. Thus, the binding free energy calculation/decomposition were employed to analyze the interaction patterns between each compound and cytochrome bc1 complex. The predicted conformations of these compounds from XP model of *Glide* docking were retrieved and optimized using MM/GBSA. The detailed procedure of MM/GBSA was reported in the previous studies.[28–31] The modified GB model developed by Onufriev (GB^{OBC1}) was adopted by setting the interior (solute) dielectric constant to 1.[32] As can be seen in Table 3, the binding free energies calculated by MM/GBSA has better capability than the docking scores to rank the bioactivities of this series of compounds. The compound with highest inhibition activity (compound **5s**) had the lowest binding free energy (−44.17 kcal/mol). The aligned binding

poses and interaction patterns for compounds **5s**, **5f** and positive control compound, pyraclostrobin were depicted in Fig. 2.

To uncover the contribution of key residues for inhibitor binding quantitatively, the total binding free energies for compounds **5s**, **5f** and pyraclostrobin were further decomposed into individual residue contributions. The inhibitor-residues interaction spectra for three compounds were illustrated in Fig. 3. Apparently, minor chemical modifications could induce different binding poses for in the binding pocket. For example, the pyridine ring in compound **5s** can form stable arene-H interaction with residue proline 271 (Figs. 2d and 3). Whereas, this interaction cannot be observed between pyraclostrobin and cytochrome bc1 complex. The result demonstrated that the activity difference was not simply caused by the pyridine ring. Similar phenomenon can also be observed for compounds **5s** and **5f** (Fig. 2c and d). The predicted total binding free energies for compounds **5s**, **5f** and pyraclostrobin were −44.17, −23.84 and −35.85 kcal/mol, respectively. The major differences among three compounds, especially between compounds **5s** and **5f** were the contributions of six key residues including Met125, Phe129, Gly143, Pro271, Glu272 and Phe275. The differences for these residues between the compounds **5s** and **5f** were higher than 1.0 kcal/mol. This observation is consistent with the finding derived from *Glide* docking. As can be shown in Fig. 1c and d, the important interactions between the inhibitor and residue such as Met125, Glu272 and Phe275 were broken by replacing the R group (4-methylene-1,1′-biphenyl) of compound **5s** with the R group (1,1′-biphenyl) of compound **5f**. Consequently, retention the interaction between pyridine in compound **5s** and proline 271, while modification the R group of this series of compounds to achieve improved interaction with positive key residues, like Met125 and Phe 275 (Fig. 3) might produce more potent inhibitors in the next lead optimization stage.

Finally, the observed decreased potency for several compounds in cellular relative to enzymatic assay is noticed. It was understood to be the consequence of compound permeability, or could be the competition with endogenous substrates, et al. This so called rightward shift in potency is commonly reported.[33]

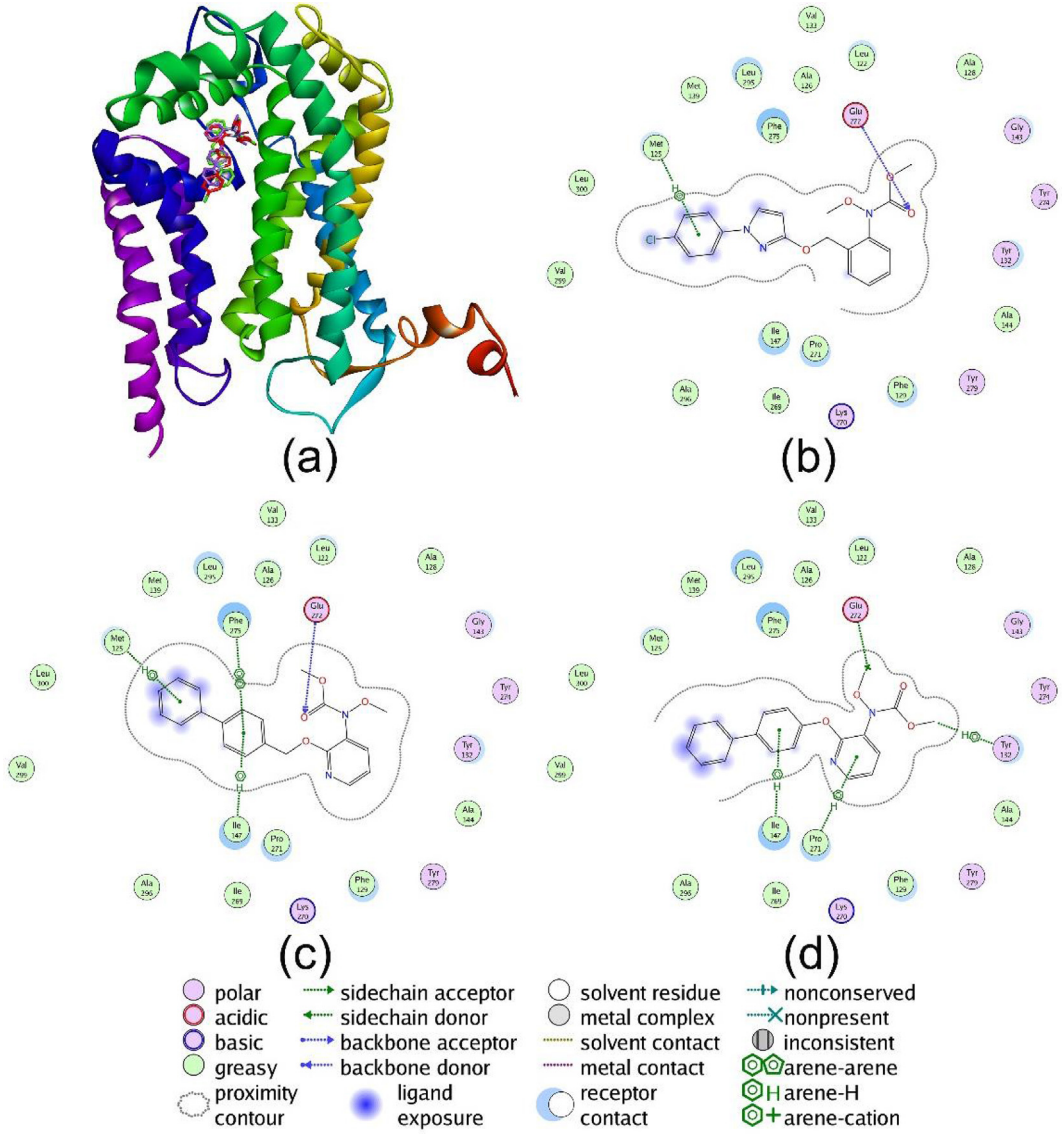

Fig. 2. (a) The aligned predicted binding poses for compound **5s** (colored in green), **5f** (colored in purple) and positive control compound, pyraclostrobin (colored in red) in the binding pocket of cytochrome bc1 complex. The interaction patterns predicted by *Glide* docking and MM/GBSA minimization for (b) positive control compound, pyraclostrobin; (c) compound **5s**; (d) compound **5f**.

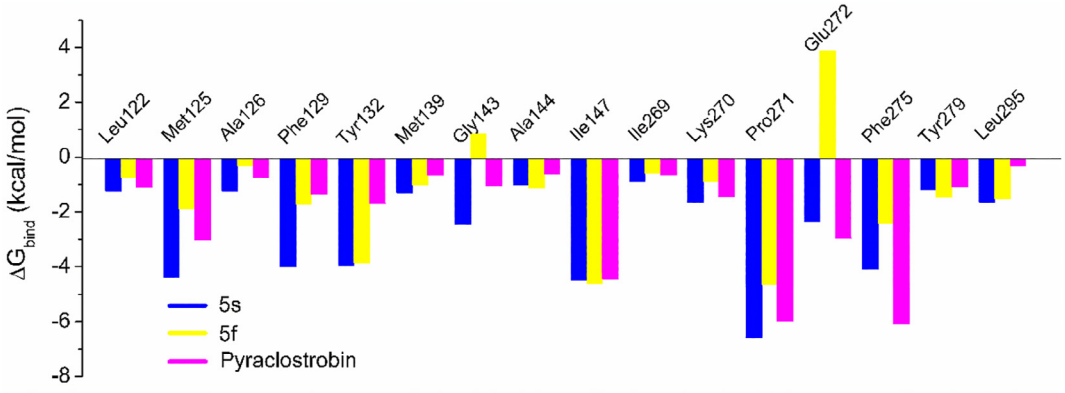

Fig. 3. The inhibitor-residues interaction spectra for compounds **5s**, **5f** and positive control compound, pyraclostrobin.

3. Conclusion

In summary, a series of novel pyraclostrobin analogues were designed and prepared using a convenient synthetic route. The in vitro antifungal assay result indicated that eight out of twenty-three compounds displayed significant inhibitory activity against five selected phytopathogenic fungal strains and their antifungal activities are comparable to that of positive control pyraclostrobin. Although only one analogue reported herein was found to possess lower IC_{50} against porcine SCR than pyraclostrobin, our results confirmed that some analogues, especially typeΠseries, inhibited the activities of SCR from porcine heart mitochondria. The combined computational strategy was applied to calculate binding free energy and key favorable residues for inhibitor binding were discerned. On the basis of our present experiment results, several suggestions for further structural modification of the pyridinyl linker pyraclostrobin analogues could be put forward: hydrophobic side chain is critical for the compound antifungal activity, biaryl rings at the side chain is preferable, appropriate flexibility is beneficial to the inhibitory activity against bc_1 complex. Finally, the antifungal activity of these compounds against pyraclostrobin resistant phytopathogenic fungi are under investigation and deserves further exploration.

Acknowledgements

The National Key Research and Development Program of China (2017YFD0200506). We also thank Prof. Guangfu Yang from Central China Normal University for the SCR experiments.

A. Supplementary data

Supplementary data associated with this article can be found, in the online version, at https://doi.org/10.1016/j.bmc.2018.01.004.

References

1. Karadimos DA, Karaoglanidis GS, Tzavella-Klonari K. Biological activity and physical modes of action of the Q_o inhibitor fungicides trifloxystrobin and pyraclostrobin against *Cercospora beticola*. *Crop Prot*. 2005;24:23–29.
2. Esser L, Quinn B, Li YF, et al. Crystallographic studies of quinol oxidation site inhibitors: a modified classification of inhibitors for the cytochrome bc1 complex. *J Mol Biol*. 2004;341:281–302.
3. Bartlett DW, Clough JM, Godwin JR, Hall AA, Hamer M, Parr-Dobrzanski B. The strobilurin fungicides. *Pest Manag Sci*. 2002;58:649–662.
4. Fisher N, Meunier B. Re-examination of inhibitor resistance conferred by Q_o-site mutations in cytochrome *b* using yeast as a model system. *Pest Manag Sci*. 2005;61:973–978.
5. Markoglou AN, Malandrakis AA, Vitoratos AG, Ziogas BN. Characterization of laboratory mutants of *Botrytis cinerea* resistant to Q_oI fungicides. *Eur J Plant Pathol*. 2006;115:149–162.
6. Abreu SDM, Caboni P, Cabras P, Garau VL, Alves A. Validation and global uncertainty of a liquid chromatographic with diode array detection method for the screening of azoxystrobin, kresoxim-methyl, trifloxystrobin, famoxadone, pyraclostrobin and fenamidone in grapes and wine. *Anal Chim Acta*. 2006;573–574:291–297.
7. Zhang X, Liu HJ, Gao YX, Wang HL, Guo BY, Li JZ. Synthesis and antifungal activities of new type *β*-methoxyacrylate-based strobilurin analogues. *Chinese J Chem*. 2012;30:1517–1524.
8. Li Y, Zhang HQ, Liu J, Yang XP, Liu ZJ. Stereoselective synthesis and antifungal activities of (*E*)-α-(methoxyimino)benzeneacetate derivatives containing 1,3,5-substituted pyrazole ring. *J Agric Food Chem*. 2006;54:3636–3640.
9. Li M, Liu CL, Yang JC, et al. Synthesis and biological activity of new (*E*)-α-(methoxyimino) benzeneacetate derivatives containing a substituted pyrazole ring. *J Agric Food Chem*. 2010;58:2664–2667.
10. Huang W, Zhao PL, Liu CL, Chen Q, Liu ZM, Yang GF. Design, synthesis, and fungicidal activities of new strobilurin derivatives. *J Agric Food Chem*. 2007;55:3004–3010.
11. Tu S, Xu LH, Ye LY, Wang X, Sha Y, Xiao ZY. Synthesis and fungicidal activities of novel indene-substituted oxime ether strobilurins. *J Agric Food Chem*. 2008;56:5247–5253.
12. Zhang X, Gao YX, Liu HJ, Guo BY, Wang HL. Design, synthesis and antifungal activities of novel strobilurin derivatives containing pyrimidine moieties. *Bull Korean Chem Soc*. 2012;33:2627–2634.
13. Zhu XL, Wang F, Li H, Yang WC, Chen Q, Yang GF. Design, synthesis, and bioevaluation of novel strobilurin derivatives. *Chin J Chem*. 2012;30:1999–2008.
14. Li M, Liu CL, Li L, et al. Design, synthesis and biological activities of new strobilurin derivatives containing substituted pyrazoles. *Pest Manag Sci*. 2010;66:107–112.
15. Aspinall IH, Worthington PA. *β*-Methoxyacrylates; synthesis of new types of strobilurin fungicides with extended side chains. *Pestic Sci*. 1999;55:197–198.
16. Liu HJ, Zhang X, Gao YX, Li JZ, Wang HL. Design, synthesis, and antifungal activities of new β-methoxyacrylate analogues. *J Chin Chem Soc*. 2013;60:27–34.
17. Liu CL, Guan AY, Yang JD, et al. Efficient approach to discover novel agrochemical candidates: intermediate derivatization method. *J Agric Food Chem*. 2016;64:45–51.
18. Liu AP, Wang XG, Ou XM, et al. Synthesis and fungicidal activities of novel bis (trifluoromethyl)phenyl-based strobilurins. *J Agric Food Chem*. 2008;56:6562–6566.
19. Liu AP, Wang XG, Chen C, et al. The discovery of HNPC-A3066: a novel strobilurin acaricide. *Pest Manag Sci*. 2009;65:229–234.
20. Sridhara AM, Reddy KRV, Keshavayya J, et al. Synthesis, antimicrobial and cytotoxicity studies of some novel modified strobilurin derivatives. *J Brazil Chem Soc*. 2011;22:849–856.
21. Sridhara AM, Reddy KRV, Keshavayya J, et al. Synthesis, antimicrobial and cytotoxicity studies of some novel phthalazine-methoxyacrylate derivatives. *J Pharm Res*. 2011;4:496–500.
22. Tong JH, Wang HY, Cai XD, Zhang QP, Ma HC, Lei ZQ. Suzuki coupling reaction catalyzed heterogeneously by Pd(salen)/polyoxometalate compound: another example for synergistic effect of organic/inorganic hybrid. *Appl Organomet Chem*. 2014;28:95–100.
23. Edsall RJ, Harris HA, Manas ES, Mewshaw RE. $ER_β$ ligands. Part 1: the discovery of ERβ selective ligands which embrace the 4-hydroxy-biphenyl template. *Bioorg Med Chem*. 2003;11:3457–3474.
24. Winter C, Rheinheimer J, Wolf A, et al. Preparation of strobilurin type compounds for combating phytopathogenic fungi. PCT Int. Appl. WO 2014202703 A1 20141224.

25. Chen Y, Zhuo ZJ, Cui DM, Zhang C. Copper catalyzed synthesis of 1-aryl-1,2,3-triazoles from aryl iodides, alkynes, and sodium azide. *J Organomet Chem*. 2014;749:215–218.
26. Chan WL, Ding M, Zou B. Preparation of spiropyrazolopyridine derivatives and uses thereof for the treatment of viral infections. PCT Int. Appl. WO 2014167528 A1 20141016. 2014.
27. Zhu Xiaolei, Zhang Mengmeng, Liu Jingjing, Ge Jingming, Yang Guangfu. Ametoctradin is a potent Q_0 site inhibitor of mitochondrial respiration complex III. *J Agric Food Chem*. 2015;63:3377–3386.
28. Hou T, Wang J, Li Y, Wang W. Assessing the performance of the MM/PBSA and MM/GBSA methods. 1. The accuracy of binding free energy calculations based on molecular dynamics simulations. *J Chem Inf Model*. 2011;51:69–82.
29. Hou T, Wang J, Li Y, Wang W. Assessing the performance of the molecular mechanics/poisson boltzmann surface area and molecular mechanics/generalized born surface area methods. II. The accuracy of ranking poses generated from docking. *J Comput Chem*. 2011;32:866–877.
30. Sun H, Li Y, Tian S, Xu L, Hou T. Assessing the performance of MM/PBSA and MM/GBSA methods. 4. Accuracies of MM/PBSA and MM/GBSA methodologies evaluated by various simulation protocols using PDBbind data set. *PCCP*. 2014;16:16719–16729.
31. Chen F, Liu H, Sun H, et al. Assessing the performance of the MM/PBSA and MM/GBSA methods. 6. Capability to predict protein-protein binding free energies and re-rank binding poses generated by protein-protein docking. *PCCP*. 2016;18:22129–22139.
32. Onufriev A, Bashford D, Case DA. Exploring protein native states and large-scale conformational changes with a modified generalized born model. *Proteins Struct Funct Bioinf*. 2004;55:383–394.
33. Schwaid AG, Cornella-Taracido I. Causes and significance of increased compound potency in cellular or physiological contexts. *J Med Chem*. 2017. https://doi.org/10.1021/acs.jmedchem.7b00762.